TTP 95-12‡
March 1995
hep-ph/9503461

Polarized Heavy Quarks *

Marek Jeżabek **
Institute of Nuclear Physics, Kawiory 26a, PL-30055 Cracow, Poland
and
Institut für Theoretische Teilchenphysik, D-76128 Karlsruhe, Germany

Abstract

Polarization studies for heavy quarks can lead to important tests of the Standard Model. Top quark pair production in e^+e^- annihilation is considered near energy threshold. It is shown that for longitudinally polarized electrons the produced top quarks and antiquarks are highly polarized. Dynamical effects originating from strong interactions in the $t-\bar{t}$ system can be calculated using Green function method. Energy-angular distributions of leptons in semileptonic decays of polarized heavy quarks are sensitive to both the polarization of the decaying quark and V-A structure of the weak charged current. Some applications to b quark physics at the Z^0 resonance are briefly reviewed.

To be published in Acta Physica Polonica B
Proceedings of the Cracow Epiphany Conference on Heavy Quarks
Jan.5-6, 1995, Cracow, Poland
In honour of the 60th birthday of Kacper Zalewski

‡The complete preprint, including figures, is also available via anonymous ftp at ttpux2.physik.uni-karlsruhe.de (129.13.102.139) as /ttp95-12/ttp95-12.ps, or via www at http://ttpux2.physik.uni-karlsruhe.de/cgi-bin/preprints/

*Work supported in part by KBN grant 2P30225206 and by DFG.

** Alexander-von-Humboldt Foundation fellow.

1 Introduction

Polarization plays a crucial role in physics of electroweak interactions. Starting from the fifties when parity violation was discovered up to present days of the LEP [1, 2] and SLC [3] experiments, polarized fermions in initial and final states have been instrumental in uncovering properties of fundamental particles and their interactions. Quite often due to a large degree of polarization, high accuracy can be achieved even for a relatively low number of events. A recent spectacular example is the precise measurement of the electroweak mixing parameter $\sin^2\theta_{\rm w}^{eff}$ at SLC [4]. Nowadays many processes involving polarized leptons are successfully employed at experimental facilities. The situation is quite opposite for the strongly interacting fundamental fermions. Due to confinement the quarks remain bound inside hadrons which are strongly interacting composite systems. Thus in general the physical quantities depend on the polarizations of quarks in intricate manner. It is remarkable, however, that Nature provides us with a few processes which can be considered as sources of highly polarized top, bottom, and charm quarks. Moreover, in these reactions the polarizations of the heavy quarks are not much affected by strong interactions. Some physicists believe that the third generation of quarks is the best available window on new physics beyond the Standard Model. Therefore, it is reasonable to expect that future experimental studies with polarized heavy quarks will lead to significant progress in particle physics.

In the present article some reactions are discussed which involve polarized heavy quarks. In Sect.2 sources of polarized top quarks are discussed. In Sect.3 top quark pair production in e^+e^- annihilation is considered near production threshold. It is shown that the Green function method [5, 6, 7, 8] can be extended to the case of polarized t and $\bar{t}$. Some results of our recent studies [9, 10] are presented. In particular it has been demonstrated that for the longitudinally polarized electron beam an optimally polarized sample of top quarks can be produced. In Sect.4 semileptonic decays of heavy quarks are discussed including recent results on QCD corrections to these processes. We argue that the cleanest spin analysis for the top quarks can be obtained from their semileptonic decay channels. In Sect.5 polarization phenomena for b and c quarks produced at the Z^0 peak are briefly reviewed.

2 Sources of polarized heavy quarks

As the heaviest fermion of the Standard Model the top quark is an exciting new window on very high mass scale physics. There is no doubt that precise studies of top quark production and decays will provide us with new information about the mechanism of electroweak symmetry breaking. The analysis of polarized top quarks and their decays has recently attracted considerable attention; see [11, 12] and references cited therein. For non-relativistic top quarks the polarization studies are free from hadronization ambiguities. This is due to the short lifetime of the top quark which is shorter than the formation time of top mesons and toponium resonances. Therefore top decays intercept the process of hadronization at an early stage and practically eliminate associated non-perturbative effects.

Many processes have been proposed which can lead to the production of polarized top quarks. In hadronic collisions and for unpolarized beams the polarization studies are mainly based on the correlation between t and $\bar{t}$ decay products. However, single top production through Wb fusion at LHC may also be a source of polarized top quarks. An interesting reaction is top quark pair production in $\gamma\gamma$ annihilation at a linear photon collider. At such a machine the high energy photon beams can be generated via Compton scattering of laser light on electrons accelerated in the linac. The threshold behaviour of the reaction $\gamma\gamma \to t\bar{t}$ has been reviewed in [13] and the top quark polarization in this reaction has been recently considered in [14]. A linear photon collider is a very interesting project. If built it may prove to be one of the most useful facilities exploring the high energy frontier. However, at present it is not clear whether the energy resolution of this accelerator can be considerably improved. As it stands the energy resolution limits precision of the top quark threshold studies at photon colliders. The most efficient and flexible reaction producing polarized top quarks is pair production in e^+e^- annihilation with longitudinally polarized electron beams. For $e^+e^- \to t\bar{t}$ in the threshold region one can study decays of polarized top quarks under particularly convenient conditions: large event rates, well-identified rest frame of the top quark, and large degree of polarization. At the same time, thanks to the spectacular success of the polarization program at SLC [3], the longitudinal polarization of the electron beam will be an obvious option for a future linear collider.

3 Top quark pair production near threshold

3.1 Green function method

The top quark is a short–lived particle. For the top mass m_t in the range 160–190 GeV its width Γ_t increases with m_t from 1 to 2 GeV. Thus Γ_t by far exceeds the tiny ($\sim$ 1 MeV) hyperfine splitting for toponia and open top hadrons, the hadronization scale of about 200 MeV, and even the energy splitting between $1S$ and $2S$ $t\bar{t}$ resonances. On one side this is an advantage because long-distance phenomena related to confinement are less important for top quarks [15, 16]. In particular depolarization due to hadronization is practically absent. On the other side the amount of information available from the threshold region is significantly reduced. Toponium resonances including the $1S$ state overlap each other. As a consequence the cross section for $t\bar{t}$ pair production near energy threshold has a rather simple and smooth shape.

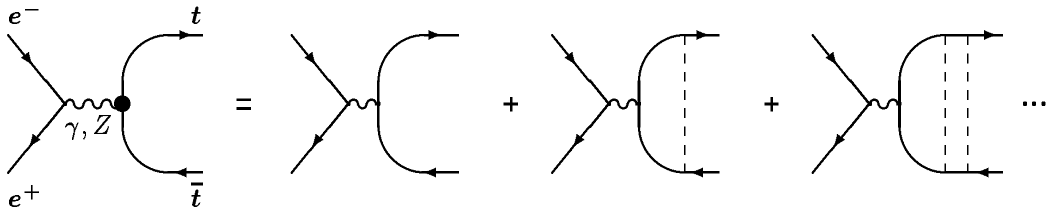

Figure 1: Dominant contributions to the process $e^+e^- \to t\bar{t}$ near threshold.

The quantitative theoretical study of the threshold region is a complicated problem. The excitation curve $\sigma(e^+e^- \to t\bar{t})$ depends on m_t and Γ_t. In addition it is drastically affected by strong interactions. A few GeV below and above the nominal threshold $\sqrt{s} = 2m_t$ a multitude of overlapping S wave resonances is excited. One might think that a reasonably accurate description can be obtained by performing a sum over these resonances. However, it has been shown [17] that one has to include so many resonances that such an approach is practically useless. Perturbative approach is also non-trivial in the threshold region. In seminal papers [5] Fadin and Khoze have demonstrated that for non-relativistic t and $\bar{t}$ the dominant contribution to the amplitude is given by the sum of the ladder diagrams depicted in Fig.1. The dashed lines denote the instantaneous parts of the gluon propagators which in the Coulomb gauge read

$$D^{\mu\nu}\left(q^2\right) \sim \delta^{\mu 0}\delta^{\nu 0} V(\mathbf{q}) \tag{1}$$

where $\mathbf{q}$ denotes the three-momentum transfer and $V(\mathbf{q})$ is the chromostatic potential in the momentum space. We have also neglected contributions of space-space components D^{ij} which are suppressed by factors of order β^2. The diagram with n exchanges gives the contribution of order $(\alpha_s/\beta)^n$ where α_s is the strong coupling constant and β denotes the velocity of the top quark in the center-of-mass frame. In the threshold region $\beta \sim \alpha_s$ and all the contributions are of the same order. In [5] it has been also shown that the sum of the terms in Fig.1 can be expressed through the Green function of the $t-\bar{t}$ system. The effects of the top quark width have been incorporated through the complex energy $E + i\Gamma_t$, where

$$E = \sqrt{s} - 2m_t$$

is the non-relativistic energy of the system. Finally, Fadin and Khoze [5] have calculated analytically the Green function for the Coulomb chromostatic interaction between t and $\bar{t}$. They have pointed out that the excitation curve $\sigma(e^+e^- \to t\bar{t})$ allows a precise determination of m_t as well as of other quantities such as Γ_t and α_s. Strassler and Peskin [6] have obtained similar results using a numerical approach and a more realistic QCD potential. The idea [5, 6] to use the Green function instead of summing over overlapping resonances has been also applied in numerical calculations of differential cross sections. Independent approaches have been developed for solving Schrödinger equation in position space [8] and Lippmann-Schwinger equation in momentum space [7, 18]. The results of these two methods agree very well [19]. One of the most important future applications will be the determination of m_t and α_s. More detailed discussions can be found in the original papers and in the recent reviews [11, 12, 13, 20].

3.2 Vertices and Lippmann-Schwinger equations

It has been already mentioned that the hyperfine splitting for $t-\bar{t}$ system is much smaller than its lifetime. This implies that the polarizations of t and $\bar{t}$ are only weakly affected by QCD interactions between these quarks. It is natural, therefore, to consider the production of t quark (and $\bar{t}$ antiquark) of given polarization. For the sake of simplicity we confine our discussion to the case of top quark polarization. Two-particle spin correlations for the $t-\bar{t}$ system will be discussed elsewhere [10]. In close analogy to the unpolarized case, c.f. Fig.1, we consider e^+e^- annihilation into $t\bar{t}$ pair. The four-momentum of the top quark is denoted by p_+ and its spin four-vector by s_+. The antiquark $\bar{t}$ carries the four-momentum p_-. The electron and the positron are relativistic and their masses can be neglected. Let $k_\pm$ denote the four-momenta of $e^\pm$ ($k_\pm^2 = 0$),

$$Q \;=\; k_- \;+\; k_+ \;=\; \left(\sqrt{s}, 0, 0, 0\right)$$

and

$$K \;=\; k_- \;-\; k_+ \;=\; \left(0, 0, 0, \sqrt{s}\right)$$

The matrix element squared for $e^+e^- \to t\bar{t}$ can be written as a contraction of the leptonic and hadronic tensors

$$|\mathcal{M}|^2 \;\sim\; L^{\alpha\beta}\, H_{\alpha\beta} \tag{2}$$

It is evident from Fig.1 that the leptonic tensor $L^{\alpha\beta}$ is well described by the Born expression whereas the hadronic tensor $H_{\alpha\beta}$ is given by a complicated sum of ladder diagrams. Let J_z denote the component of the total angular momentum in the direction of e^-. Then

$$L^{\alpha\beta} = 0 \quad \text{for} \quad J_z = 0$$

whereas for for $J_z = \pm 1$

$$\begin{aligned} L^{\alpha\beta}_{VV} \;&=\; L^{\alpha\beta}_{AA} \;&=\;& L^{\alpha\beta}_{s} \;+\; J_z\, L^{\alpha\beta}_{a} \\ L^{\alpha\beta}_{VA} \;&=\; L^{\alpha\beta}_{AV} \;&=\;& J_z\, L^{\alpha\beta}_{s} \;+\; L^{\alpha\beta}_{a} \end{aligned} \tag{3}$$

The subscripts A and V denote the contributions of the vector and axial-vector leptonic currents, and

$$\begin{aligned} L^{\alpha\beta}_{s} \;&\sim\; s g^{\alpha\beta} - Q^\alpha Q^\beta + K^\alpha K^\beta \\ L^{\alpha\beta}_{a} \;&\sim\; \varepsilon^{\alpha\beta\lambda\mu} Q_\lambda K_\mu \end{aligned} \tag{4}$$

It follows from eq.(3) that for longitudinally polarized electrons and positrons the total annihilation cross section is proportional to

$$1 - P_{e^+} P_{e^-}$$

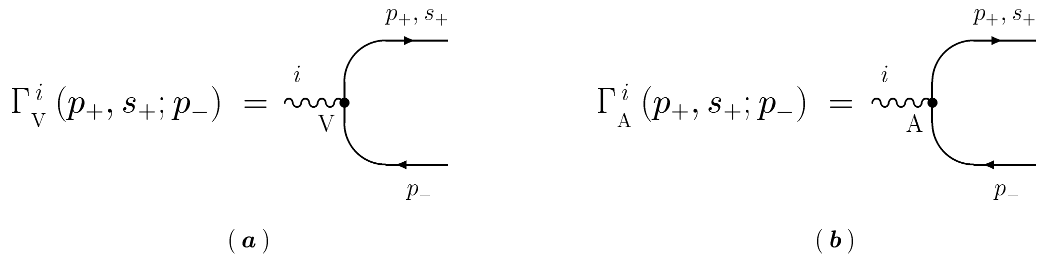

Figure 2: Effective vertices describing the couplings of a) the vector and b) the axial-vector current to the top quark of four-momentum p_+ and spin four-vector s_+ and the antiquark $\bar{t}$ of four-momentum p_-.

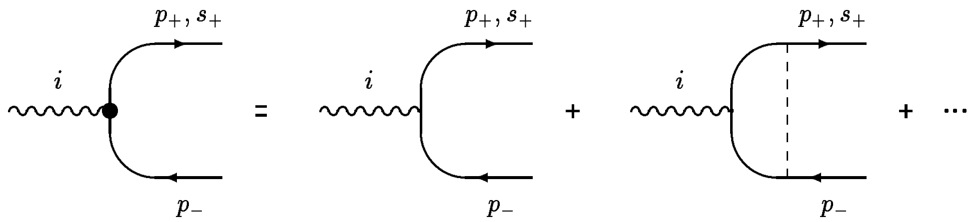

Figure 3: Definition of the effective vertices.

where P_{e^+} and P_{e^-} denote the polarizations of e^+ and e^-, with respect to the directions of e^+ and e^- beams, respectively. Furthermore, the polarization of the top quark depends only on the variable

$$\chi = \frac{P_{e^+} - P_{e^-}}{1 - P_{e^+} P_{e^-}} \tag{5}$$

It is conceivable that for a future linear e^+e^- collider $P_{e^+} = 0$, $P_{e^-} \neq 0$ and $\chi = -P_{e^-}$. Another interesting observation is that only the space-like components H^{ij} of the hadronic tensor can contribute to the differential cross section. (In fact only the transverse components $i, j = 1, 2$ give non-zero contributions.) Thus in the following discussion we consider only the components H^{ij} of the hadronic tensor.

In the center-of-mass frame the velocity of the top quark is small ($\beta = |\mathbf{p}|/m_t \ll 1$) and we can use the non-relativistic approximation for t and $\bar{t}$. The spin four-vector is

$$s_+^\mu = (0, \mathbf{s}_+) + \mathcal{O}(\beta) \tag{6}$$

Thus, up to terms of order β^2 the spin three-vector $\mathbf{s}_+$ is the same as in the top quark rest frame. We define effective vertices Γ^i_V and Γ^i_A describing the couplings of the vector (V) and the axial-vector currents (A) to the top quark of four-momentum p_+ and spin four-vector s_+ and the antiquark $\bar{t}$ of four-momentum p_-, see Fig.2. Each of these vertices is an infinite sum of ladder diagrams corresponding to instantaneous Coulomb-like exchanges of gluons between t and $\bar{t}$, see Fig.3. The space-like components of the hadronic tensor H^{ij} can be expressed through the effective vertices

$$H^{ij} \sim \sum_{a,b} Tr \left[\Gamma^i_a \widetilde{\Gamma^j_b} \right] \tag{7}$$

where $a, b = V, A$ and $\widetilde{O} = \gamma^0 O^\dagger \gamma^0$. Let us define now the projection operators

$$\Lambda_\pm = \tfrac{1}{2} \left(1 \pm \gamma^0 \right) \tag{8}$$

We can split any operator O into two pieces $(O)_\pm$:

$$\begin{aligned} (O)_+ &= \Lambda_+ O \Lambda_+ + \Lambda_- O \Lambda_- \\ (O)_- &= \Lambda_+ O \Lambda_- + \Lambda_- O \Lambda_+ \end{aligned} \tag{9}$$

which we call even and odd parts of O respectively. It can be shown that

$$\Gamma^i_V = \left(\Gamma^i_V \right)_- + \mathcal{O}(\beta) \qquad \text{and} \qquad \Gamma^i_A = \mathcal{O}(\beta) \tag{10}$$

Any product of an odd and an even operator is traceless, so up to terms of order β^2 only odd parts of Γ^i_a can contribute to H^{ij}.

$$H^{ij} \sim \sum_{a,b} Tr \left[(\Gamma^i_a)_- (\widetilde{\Gamma^j_b})_- \right] + \mathcal{O}\left(\beta^2 \right) \tag{11}$$

Furthermore, with the same accuracy the effective vertices can be expressed through two scalar functions: $\mathcal{K}_V(p, E)$ and $\mathcal{K}_A(p, E)$ where $p = |\mathbf{p}|$. It follows from Fig.3 that

$$\left(\Gamma^j_V(p_+, s_+; p_-) \right)_- = \Lambda_+ \Sigma_+ \gamma^j \Lambda_- \, \mathcal{K}_V(p, E) \tag{12}$$

$$\left(\Gamma^j_A(p_+, s_+; p_-) \right)_- = \frac{i}{m_t} \Lambda_+ \Sigma_+ (\vec{\gamma} \times \mathbf{p})^j \Lambda_- \, \mathcal{K}_A(p, E) \tag{13}$$

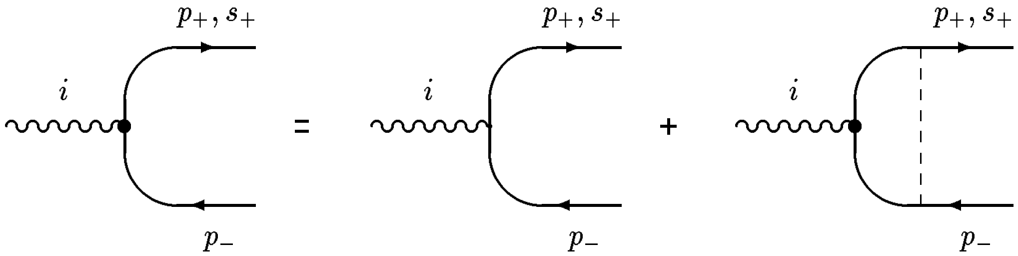

Figure 4: Lippmann–Schwinger equation for the effective vertices.

where

$$\Sigma_+ \; = \; \tfrac{1}{2}\,(1 + \mathbf{s}_+ \cdot \mathbf{\Sigma}) \tag{14}$$

and $\Sigma^i \; = \; \gamma_5\,\gamma^0\,\gamma^i$ is the Dirac spin operator. The series defining the effective vertices, see Fig.3, can be formally summed. In this way the equation depicted in Fig.4 is derived. Neglecting the corrections of order β^2 one obtains the following integral equations for the functions $\mathcal{K}_V\,(p, E)$ and $\mathcal{K}_A\,(p, E)$

$$\mathcal{K}_V\,(p, E) \;\; = \;\; 1 + \int \frac{d^3 q}{(2\pi)^3}\, V\,(\mathbf{p} - \mathbf{q})\, G_0(q, E)\, \mathcal{K}_V\,(q, E) \tag{15}$$

$$\mathcal{K}_A\,(p, E) \;\; = \;\; 1 + \int \frac{d^3 q}{(2\pi)^3}\, \frac{\mathbf{p} \cdot \mathbf{q}}{p^2}\, V\,(\,\mathbf{p} - \mathbf{q})\, G_0(q, E)\, \mathcal{K}_A\,(q, E) \tag{16}$$

where $G_0(p, E)$ is the free Green function for the $t - \bar{t}$ system[1]

$$G_0(p, E) \; = \; \frac{-1}{2\pi i} \int \frac{dp^0}{\left(p^0 - \frac{\mathbf{p}^2}{2m_t} + \mathrm{i}\frac{\Gamma_t}{2}\right)\left(E - p^0 - \frac{\mathbf{p}^2}{2m_t} + \mathrm{i}\frac{\Gamma_t}{2}\right)} \; = \; \frac{1}{E - \frac{\mathbf{p}^2}{m_t} + \mathrm{i}\Gamma_t} \tag{17}$$

It can be shown that the function

$$G(p, E) \;\; = \;\; G_0(p, E)\, \mathcal{K}_V\,(p, E) \tag{18}$$

[1] It is consistent to neglect the momentum dependence of the width for the non-relativistic $t - \bar{t}$ system because the corresponding corrections are of order β^2. Recent measurements by CDF collaboration[22] imply $m_t = 176 \pm 8(stat.) \pm 10(sys.)$ GeV and the analysis of DØ collaboration[23] gives $199^{+19}_{-21}(stat.) \pm 22(sys.)$ GeV. It has been shown that the corrections due to momentum dependent width cancel to large extent and are quite small for $m_t \sim 180$ GeV [18, 25].

is the S wave Green function [5, 6]. It solves the following Lippmann-Schwinger equation

$$G\,(p,E) = G_0(p,E) \;+\; G_0(p,E)\int \frac{d^3q}{(2\pi)^3}\, V\,(\mathbf{p}-\mathbf{q})\; G(q,E) \tag{19}$$

which follows trivially from eq.(15). The function

$$F(p,E) \;=\; G_0(p,E)\,\mathcal{K}_A\,(p,E) \tag{20}$$

is related to the P wave Green function [21]. The Lippmann-Schwinger equation for $F(p,E)$ follows from eq.(16):

$$F\,(p,E) = G_0(p,E) \;+\; G_0(p,E)\int \frac{d^3q}{(2\pi)^3}\,\frac{\mathbf{p}\cdot\mathbf{q}}{p^2}\, V\,(\mathbf{p}-\mathbf{q})\; F(q,E) \tag{21}$$

A remarkable feature of the odd parts of the effective vertices $\Gamma^j_V(p_+,s_+;p_-)$ and $\Gamma^j_A(p_+,s_+;p_-)$ is that in non-relativistic approximation their spinor structures are not changed by chromostatic interactions, see eqs.(12) and (13). When these interactions are switched off (i.e. $V=0$) the sums of the ladder diagrams which define the effective vertices reduce to single diagrams with no gluon exchanges, the vertex functions $\mathcal{K}_V\,(p,E)$ and $\mathcal{K}_A\,(p,E)$ become equal one, and the spinor structures remain the same. This means that from a practical point of view the calculations of the matrix element squared (2) including chromostatic interactions between t and $\bar{t}$ can be reduced to the evaluation of Born contributions. The only difference is that the vector and axial-vector couplings g_v and g_a of the quark current to photon and Z^0 are modified:

$$g_v \;\to\; \tilde{g}_v = g_v(4m_t^2)\left(1-\tfrac{8\alpha_s}{3\pi}\right)\mathcal{K}_V\,(p,E) \tag{22}$$

$$g_a \;\to\; \tilde{g}_a = g_a(4m_t^2)\left(1-\tfrac{4\alpha_s}{3\pi}\right)\mathcal{K}_A\,(p,E) \tag{23}$$

The prescription given in eqs.(22) and (23) includes not only chromostatic interactions but also two other important effects: the scale dependence of the running coupling constants $g_{v,a}(4m_t^2)$ and the factors $(1-8\alpha_s/3\pi)$ and $(1-4\alpha_s/3\pi)$ which arise from loop integrations over the relativistic region (contributions of hard transverse gluons); see [6] and [24].

3.3 Cross sections

We are ready now to describe the process which consists of the emission of a $t - \bar{t}$ system by a virtual photon or Z^0 and its subsequent propagation and decay into $\bar{t}W^+b$ (or $tW^-\bar{b}$). This is just the most difficult part of the calculation for which perturbative (in α_s) approach is not adequate. After the decay the time evolution of the system is governed by the free motion of W^+ and chromodynamical interactions in the $\bar{t} - b$ system. (If $\bar{t}$ decays first one considers the analogous time evolution for W^- and $t - \bar{b}$). In this period one of the strongly interacting fermions is relativistic. In contrast to the case of the $t - \bar{t}$ system the summation over ladder diagrams is not necessary because a diagram with n exchanged gluons is suppressed by α_s^n. In other words this part of the time evolution can be described in ordinary perturbative approach. Finally the $W^-\bar{t}b$ system decays into $W^-W^+\bar{b}b$. The amplitudes $\mathcal{F}_{1,2}$ describing the two decay sequences in $t - \bar{t}$ rest frame

$$\begin{aligned} \mathcal{F}_1 &: \quad \bar{t}t \to \bar{t}W^+b \to W^-W^+\bar{b}b \\ \mathcal{F}_2 &: \quad \bar{t}t \to W^-\bar{b}t \to W^-W^+\bar{b}b \end{aligned}$$

have to be added coherently. The theoretical description becomes even more complicated when W bosons are treated as unstable particles. In such a case we have six different decay sequences. Furthermore one or two of W bosons can decay into quarks whose interactions with b and/or $\bar{b}$ can be also important in some regions of phase space. These are the so-called *cross talking* or *interconnection* effects[20]. Even more important are effects of gluon radiation off $\bar{t} - b$ and $t - \bar{b}$ systems[26, 27]. All these phenomena have to be included into a complete theoretical analysis of $t\bar{t}$ production near threshold. However, it is likely that these refinements will not drastically change the results for inclusive cross sections which we consider in the following. In fact, we assume that the contributions of the interference terms cancel. This assumption can be easily justified when QCD interactions in $\bar{t}W^+b$ and $W^-\bar{b}t$ systems are neglected. Let p^0 denote the energy of t which for non-interacting system is equal to the total energy W^+b. Overall energy conservation implies that the energy of $W^-\bar{b}$ system (i.e. of $\bar{t}$) is equal to $\sqrt{s} - p^0$. The product of propagators for t and $\bar{t}$ can be written as a sum of two terms corresponding to the two different sequences of decays

$$G_0^t(p^0, \mathbf{p})\, G_0^{\bar{t}}(\sqrt{s} - p^0, -\mathbf{p}) \;=\; G_0(p, E)\, \left[G_0^{\bar{t}}(\sqrt{s} - p^0, -\mathbf{p}) \,+\, G_0^t(p^0, \mathbf{p}) \right] \quad (24)$$

where

$$G_0^t(p^0, \mathbf{p}) \;=\; G_0^{\bar{t}}(p^0, \mathbf{p}) \;=\; \frac{1}{p^0 - m_t - \frac{\mathbf{p}^2}{2m_t} + \mathrm{i}\frac{\Gamma_t}{2}} \tag{25}$$

Evidently the Fourier transform of the first term decribes time evolution of the $t - \bar{t}$ system up to the moment of t decay and the subsequent time evolution of $\bar{t}$. Thus this term corresponds to the situation when t decays before $\bar{t}$. The other term corresponds to the case when $\bar{t}$ decays before t. Neglecting some common factors we obtain the following expressions for the amplitudes $\mathcal{F}_1$ and $\mathcal{F}_2$:

$$\mathcal{F}_1 \;\sim\; G_0(p, E)\, G_0^t(p^0, \mathbf{p}) \tag{26}$$

$$\mathcal{F}_2 \;\sim\; G_0(p, E)\, G_0^{\bar{t}}(\sqrt{s} - p^0, -\mathbf{p}) \tag{27}$$

and, consequently,

$$\int dp^0 \;|\, \mathcal{F}_1 + \mathcal{F}_2 \,|^2 \;=\; \int dp^0 \;\left(|\, \mathcal{F}_1 \,|^2 + |\, \mathcal{F}_2 \,|^2 \right) \tag{28}$$

Let us consider now the effects of gluon emission and QCD interactions in $t\bar{b}$ and $b\bar{t}$ systems. As already explained the effects of rescattering for $t\bar{b}$ and $b\bar{t}$ can be included as order α_s perturbations. Other effects like real gluon emission and tbW vertex corrections decrease the top quark width Γ_t by a correction of order α_s [28, 29][2]

$$\delta\Gamma_t \;\approx\; -\Gamma_0 \, \tfrac{2\alpha_s}{3\pi} \left(\tfrac{2\pi^2}{3} - \tfrac{5}{2} - 3y \right) \tag{29}$$

where $y = m_{\mathrm{w}}^2 / m_t^2$ and

$$\Gamma_0 = \frac{G_F \, m_t^3}{8\sqrt{2}\pi} (1-y)^2 (1+2y) \tag{30}$$

The resulting reduction of the width of about[3] 10% changes significantly the time evolution of the $t\bar{t}$ system and affects the results for the total cross section

[2] The complete formula including b quark mass and W width has been obtained [28] for a free top quark. It is known [20, 26] that interference affects the gluon spectrum in $t\bar{t}$ pair production for $E_g \sim \Gamma_t$. However, $\delta\Gamma_t$ is infrared finite, so the relative correction to the width due to these effects should be only of order $\alpha_s \Gamma_t / m_t$ and can be neglected.

[3] The numerical value of $\delta\Gamma_t$ depends on the choice of the scale μ for running $\alpha_s(\mu)$. A widespread belief is that $\mu \sim m_t$ is a reasonable value. However, arguments in favour of a much lower scale $\mu = 0.12\, m_t$ have been also given in the literature[30].

in the threshold region. The rescattering corrections change the wave function ψ of $t\bar{b}$ (or $b\bar{t}$) to $\psi' = \psi + \alpha_s \delta\psi$ where up to corrections of order Γ_t/m_t the functions $\delta\psi$ and ψ are orthogonal $\int \psi \delta\psi^* = 0$ as a consequence of unitary time evolution. Thus there is no $\mathcal{O}(\alpha_s)$ contribution to the total cross section from the rescattering corrections. This fact, which was first observed long ago for the electromagnetic corrections to the lifetime of the muon bound in nuclei [31], has been recently demonstrated by explicit calculations also for the top quark pair production [32, 33]. Corrections to the differential distributions ($\sim \alpha_s \Re(\psi\delta\psi^*)$) have been calculated in [33]. The results fully confirm intuitive expectations that rescattering in $b - \bar{t}$ system leads to reduction of intrinsic momentum of $\bar{t}$ in the overall center-of-mass frame. In this frame the b quark is slowed down by the chromostatic field of $\bar{t}$. Since W^+ is colorless it propagates as a free particle. In consequence the total three-momentum of the bW^+ system decreases, which through momentum conservation implies reduction of the intrinsic momentum for $\bar{t}$. In the following discussion we neglect this correction to the top quark momentum distributions because it only weakly affects polarizations.

Throughout this article all corrections of order β^2 are systematically neglected. However, close to threshold the dependence of cross sections on the width is enhanced, so a few remarks on order α_s^2 corrections to the width of the $t - \bar{t}$ system are in order here. It has been pointed out in Ref.[8] that effects of phase space suppression are important and cannot be neglected in quantitative studies. As an example of the phase space suppression effects let us consider $t\bar{t}$ for negative non-relativistic energy $E \sim -\alpha_s^2 m_t$ and assume that t decays first. The propagator function $G_0^{\bar{t}}(\sqrt{s} - p^0, -\mathbf{p})$ is peaked for the energy of $\bar{t}$ close to the classical value. Taking into account the kinetic energies which according to virial theorem are of order $|E|$ one concludes that the invariant mass of the W^+b system is likely to be a few percent smaller than m_t. This implies an even larger reduction of the decay rate. However, it has been conjectured[18] and proven[25] that order α_s^2 rescattering corrections to the total cross section nearly cancel the negative contributions of phase space suppression. The remainder can be interpreted as due to time dilatation factors for t and $\bar{t}$ in the center-of-mass frame. Its effect on the total cross section is quite small and will be neglected in the following discussion. This implies that the volumes of the phase spaces for the W^+b and $W^-\bar{b}$ systems can be considered equal and proportional to Γ_t. In this way $\mathcal{O}(\alpha_s)$ corrections to the top width are automatically included. Integration over p^0 in eq.(28) can be easily performed

$$\int dp^0\, \Gamma_t\, |\, G_0^t(p^0, \mathbf{p})\, |^2 \;=\; \int dp^0\, \Gamma_t\, |\, G_0^{\bar t}(\sqrt{s} - p^0, -\mathbf{p})\, |^2 \;=\; 2\pi \tag{31}$$

Inclusive differential cross section for the top quark production reads

$$\frac{d\sigma(\mathbf{p}, \mathbf{s}_+)}{dp\, d\Omega} \;=\; \frac{1}{2} \left(1 + 2\, \mathcal{A}_{FB} \cos\theta + \vec{\mathcal{P}} \cdot \mathbf{s}_+ \right) \frac{d\sigma}{dp} \tag{32}$$

where $\vec{\mathcal{P}}$ characterizes the final polarization of the top quark,

$$\frac{d\sigma}{dp} \;=\; \int d\Omega \sum_{\pm \mathbf{s}_+} \frac{d\sigma(\mathbf{p}, \mathbf{s}_+)}{dp\, d\Omega} \tag{33}$$

denotes its momentum distribution, and $\mathcal{A}_{FB}$ is the forward-backward asymmetry. Collecting all the factors we obtain the following expressions:

$$\frac{d\sigma}{dp} \;=\; \frac{12\, \alpha^2 (4 m_t^2)}{s\, m_t^2} \left(1 - \tfrac{8\alpha_s}{3\pi}\right)^2 (\, 1 - P_{e^+} P_{e^-}\,)\; (a_1\, + \chi a_2)\; \Gamma_t\, |\, p\, G(p, E)\, |^2 \tag{34}$$

$$\mathcal{A}_{FB}(p, E, \chi) \;=\; \frac{a_3 + \chi a_4}{2(a_1 + \chi a_2)}\, \varphi_R(p, E) \tag{35}$$

The coefficients $a_1, \ldots, a_4$ are given in Ref.[9]. They depend on the electroweak couplings of γ and Z^0 to the electron and top quark. The function $\varphi_R(p, E)$ is defined as the real part of

$$\varphi(p, E) \;=\; \frac{\left(1 - \frac{4\alpha_s}{3\pi}\right)\; p\, F^*(p, E)}{\left(1 - \frac{8\alpha_s}{3\pi}\right) m_t\, G^*(p, E)} \tag{36}$$

Eq.(35) has been first obtained in [21] for $\chi = 0$.

The Lippmann-Schwinger equations (15) and (16) can be solved numerically using the method decribed in [7, 18]. S wave dominates the total cross section. Neglecting terms of order β^2 one obtains the following form of the optical theorem

$$\int_0^\infty dp\, p^2\, |G(p, E)\, |^2 \;=\; -\int_0^\infty dp\, p^2\, \Im\, G(p, E) \tag{37}$$

which can be used as a cross check of numerical calculations.

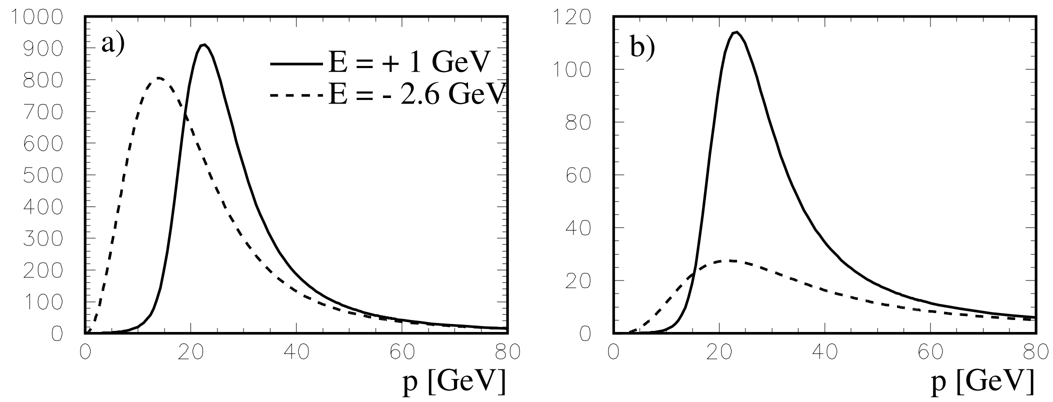

Figure 5: Top quark momentum and angular distributions for $E = 1$ and -2.6 GeV – solid/dashed lines, $m_t = 174$ GeV and $\alpha_s(m_Z) = 0.12$: a) $\mathcal{D}_{S-S}(p, E)$ and b) $\mathcal{D}_{S-P}(p, E)$.

It follows from eq.(32) that for the unpolarized electron and positron beams the momentum-angular distribution of the top quark is governed by the two functions

$$\mathcal{D}_{S-S}(p, E) = p^2 \, | \, G(p, E) \, |^2 \tag{38}$$
$$\mathcal{D}_{S-P}(p, E) = p^3 \, \Re \, (\, G(p, E) \, F^*(p, E) \,) \, / m_t \tag{39}$$

which are shown in Fig.5.

3.4 Polarizations [9, 10]

The polarization state of the top quark is given by the three-vector $\vec{\mathcal{P}}$. In an orthogonal system of coordinates we can choose any of the axes to quantize the projection of the top quark spin. This choice determines the form of the four-vector s_+ whose space component $\mathbf{s}_+$ is directed along the quantization axis and the time component is fixed by the requirement $s_+ \, p_+ = 0$. Then the projection of the polarization three-vector $\vec{\mathcal{P}}$ on the quantization axis is obtained. It is equal to the ratio of the difference and the sum of the cross sections for the spin four vectors s_+ and $-s_+$. Our righthanded system of coordinates is defined through the triplet of orthogonal unit vectors: $\hat{n}_\perp$, $\hat{n}_N$ and $\hat{n}_\parallel$ where $\hat{n}_\parallel$ points in the direction of the e^- beam, $\hat{n}_N \sim \vec{p}_{e^-} \times \vec{p}_t$ is

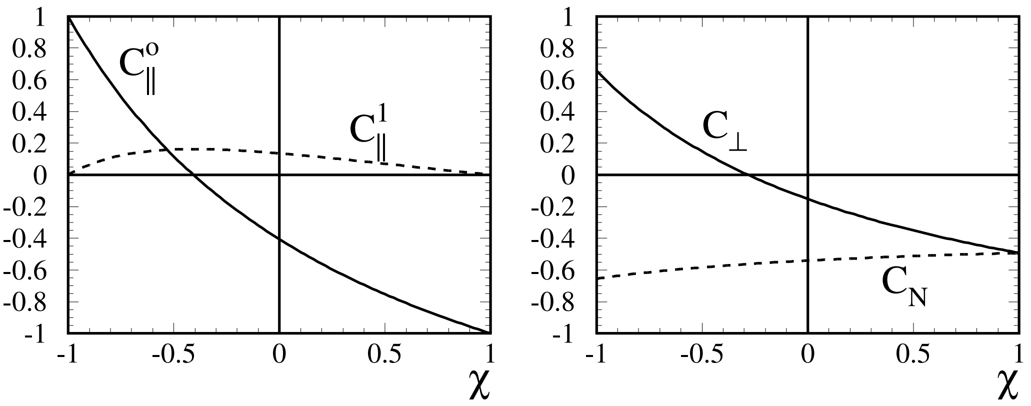

Figure 6: Coefficient functions: a) $C_\parallel^0(\chi)$ – solid line and $C_\parallel^1(\chi)$ – dashed line, b) $C_\perp(\chi)$ – solid line and $C_N(\chi)$ – dashed line.

normal to the production plane and $\hat{n}_\perp = \hat{n}_N \times \hat{n}_\parallel$. This system defines the three projections of the polarization vector $\vec{\mathcal{P}}$. The definition of $\mathcal{P}_\parallel$, $\mathcal{P}_\perp$ and $\mathcal{P}_N$ with respect to the beam direction is convenient for the treatment close to threshold and differs from the definition of [34] where the quantities have been defined with respect to the direction of flight of the top quark. The angle ϑ denotes the angle between $\hat{n}_\parallel$ and the three-momentum $\mathbf{p}$ of the top quark. As already stated in the preceding subsection we neglect rescattering corrections which will be discussed elsewhere. Retaining only the terms up to $\mathcal{O}(\beta)$ one derives the following expressions for the components of the polarization vector, as functions of E, p, ϑ and χ:

$$\mathcal{P}_\parallel(p,E,\vartheta,\chi) = C_\parallel^0(\chi) + C_\parallel^1(\chi)\,\varphi_R(p,E)\,\cos\vartheta \tag{40}$$
$$\mathcal{P}_\perp(p,E,\vartheta,\chi) = C_\perp(\chi)\,\varphi_R(p,E)\,\sin\vartheta \tag{41}$$
$$\mathcal{P}_N(p,E,\vartheta,\chi) = C_N(\chi)\,\varphi_I(p,E)\,\sin\vartheta \tag{42}$$

where $\varphi_R(p,E)$ and $\varphi_I(p,E)$ denote the real and imaginary parts of the function $\varphi(p,E)$ defined in eq.(36)

$$\varphi_R(p,E) = \Re\varphi(p,E)\ , \qquad\qquad \varphi_I(p,E) = \Im\varphi(p,E) \tag{43}$$

The energy dependence of all the coefficient functions $C(\chi)$ is very weak and can be neglected. In Fig.6a the coefficient functions $C_\parallel^0(\chi)$ and $C_\parallel^1(\chi)$ are shown. It is evident that for maximal and minimal values of $\chi = \pm 1$ the

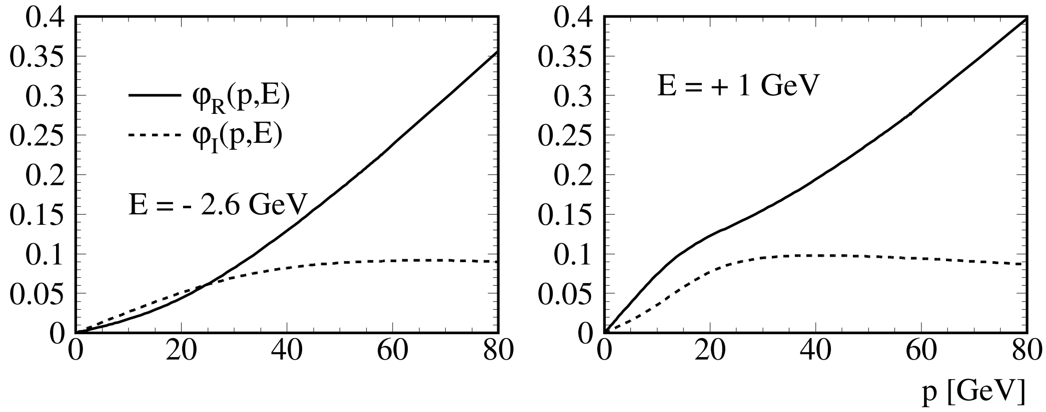

Figure 7: Momentum dependence of the functions $\varphi_R(p, E)$ (solid lines) and $\varphi_I(p, E)$ (dashed lines): a) E = -2.6 GeV, and b) E = 1 GeV.

top quark is nearly maximally polarized along the direction of the incoming electron. This demonstrates that polarization studies close to threshold are very promissing indeed. The other components of the top polarization can be also interesting and the corresponding coefficient functions are plotted in Fig.6b. Momentum dependence of the functions $\varphi_R(p, E)$ and $\varphi_I(p, E)$ is shown in Fig.7 for two energies in the threshold region.

4 Semileptonic decays of heavy quarks

The energy and angular distributions of the charged leptons and the neutrinos are sensitive to the polarization of the decaying heavy quark. Therefore they can be used in determination of this polarization. Furthermore the basic assumption about the V-A Lorentz structure of the charged weak current can be tested. In [35] compact analytic formulae have been obtained for the distributions of the charged lepton and the neutrino. These formulae agree with the energy spectra which have been obtained in [36] and also with the results of [37] and [38] for the joint angular and energy distribution of the charged lepton in top, charm and bottom quark decays. The QCD corrected triple differential distribution of the charged lepton for the semileptonic decay of the polarized quark with the weak isospin $I_3 = \pm 1/2$ can be written in the following way [35]:

$$
\begin{aligned}
\frac{\mathrm{d}\Gamma^{\pm}}{\mathrm{d}x\,\mathrm{d}y\,\mathrm{d}\cos\theta} \quad &\sim \quad \left[\mathrm{F}_0^{\pm}(x,y) + \mathcal{P}\cos\theta\,\mathrm{J}_0^{\pm}(x,y)\right] \\
&- \frac{2\alpha_s}{3\pi}\left[\mathrm{F}_1^{\pm}(x,y) + \mathcal{P}\cos\theta\,\mathrm{J}_1^{\pm}(x,y)\right]
\end{aligned}
\tag{44}
$$

In the rest frame of the decaying heavy quark θ denotes the angle between the polarization vector $\vec{\mathcal{P}}$ of the heavy quark and the direction of the charged lepton, $\mathcal{P} = |\vec{\mathcal{P}}|$, $x = 2Q\ell/Q^2$ and $y = 2\ell\nu/Q^2$ where Q, ℓ and ν denote the four-momenta of the decaying quark, charged lepton and neutrino. Eq.(44) describes also the triple differential distribution of the neutrino for $I_3 = \mp 1/2$. In this case, however, $x = 2Q\nu/Q^2$ and θ denotes the angle between $\vec{\mathcal{P}}$ and the three-momentum of the neutrino. The functions $\mathrm{F}_0^{\pm}(x,y)$ and $\mathrm{J}_0^{\pm}(x,y)$ corresponding to Born approximation read:

$$\mathrm{F}_0^{+}(x,y) = x(x_m - x) \tag{45}$$

$$\mathrm{J}_0^{+}(x,y) = \mathrm{F}_0^{+}(x,y) \tag{46}$$

$$\mathrm{F}_0^{-}(x,y) = (x-y)(x_m - x + y) \tag{47}$$

$$\mathrm{J}_0^{-}(x,y) = (x-y)(x_m - x + y - 2y/x) \tag{48}$$

where $x_m = 1 - \epsilon^2$, $\epsilon^2 = q^2/Q^2$, and q denotes the four-momentum of the quark originating from the decay. The functions $\mathrm{F}_1^{\pm}(x,y)$ and $\mathrm{J}_1^{+}(x,y)$ correspond to the first order QCD corrections and are given in [35]. Eq.(46) implies that for the top and charm quarks the double differential angular-energy distribution of the charged lepton is the product of the energy distribution and the angular distribution. QCD corrections essentially do not spoil this factorization [37]. For the neutrino such factorization does not hold, c.f. eqs.(47) and (48). After integration over x_ν the angular dependence of the neutrino distribution is much weaker than for the charged lepton. For the bottom quark the roles of the charged lepton and the neutrino are reversed. In the following part of this section we limit our discussion to the semileptonic decays of the top quark. Semileptonic decays of charm and bottom quarks will be considered in the subsequent section. For the top quark the decay rate is dominated by the mode $t \to bW^+$, so neglecting the width of W one fixes y in eq.(44) at the value $y = m_{\mathrm{w}}^2/m_t^2$.

Table 1: Angular dependence of the distributions of W bosons, neutrinos and less energetic leptons in $t \to bW \to be^+\nu$ or light quark jets in $t \to bW \to b\bar{d}u$ decays.

		m_t=150	m_t=175	m_t=200
$h_\nu(y)$	$1 - \frac{12y(1-y+y\ln y)}{(1-y)^2(1+2y)}$	-0.521	-0.311	-0.127
$h_{\rm w}(y)$	$\frac{1-2y}{1+2y}$	0.275	0.410	0.515
$h_<(y)$	$1 - \frac{6y\{1-y-2y\ln[(1+y)/(2y)]\}}{(1-y)^2(1+2y)}$	0.464	0.509	0.559

In the rest frame of the decaying t quark the angular distributions of the decay products are sensitive to its polarization. Let us define the angle $\theta_{\rm w}$ between W boson three-momentum and the polarization three-vector $\vec{\mathcal{P}}$. Note that $\mathcal{P} = |\vec{\mathcal{P}}\,| = 1$ corresponds to fully polarized and $\mathcal{P} = 0$ to unpolarized top quarks. We define also the angles θ_+ and θ_0 between $\vec{\mathcal{P}}$ and the directions of the charged lepton and the neutrino, respectively, and $\theta_<$ for the less energetic lepton in semileptonic or less energetic light quark in hadronic decays. For the sake of simplicity let us confine our discussion to Born approximation and consider semileptonic $t \to bW \to b\ell^+\nu$ and hadronic $t \to bW \to b\bar{d}u$ decays. The angular distribution of the charged lepton is of the form

$$\frac{{\rm d}N}{{\rm d}\cos\theta_+} = \frac{1}{2}\,[1\,+\,\mathcal{P}\cos\theta_+] \tag{49}$$

which follows from the factorization of the angular-energy distribution into the energy and angular dependent parts. This factorization holds for arbitrary top mass below and above the threshold for decays into real W bosons [36]. It is noteworthy that for $\mathcal{P}$=1 the angular dependence in (49) is maximal because a larger coeffecient multiplying $\cos\theta_+$ would be in conflict with positivity of the decay rate. Thus the polarization analysing power of the charged lepton angular distribution is maximal and hence far superior to other distributions discussed in the following. In particular the angular distribution of the neutrino reads [39]:

$$\frac{{\rm d}N}{{\rm d}\cos\theta_0} = \frac{1}{2}\,[1\,+\,h_\nu(y)\mathcal{P}\cos\theta_0] \tag{50}$$

where $h_\nu(y)$ is given in Table 1. The distribution of the direction of W can be easily obtained. Only the amplitudes for the helicity states of W $\lambda_{\rm w} = -1$ and $\lambda_{\rm w} = 0$ are allowed and their contributions to the decay rate are in the ratio $2y$: 1 [40]. The corresponding angular distributions are of the form

$$\frac{{\rm d}N_{-1,0}}{{\rm d}\cos\theta_{\rm w}} = \frac{1}{2}\left(1 \mp \mathcal{P}\cos\theta_{\rm w}\right) \tag{51}$$

After summation over the W polarizations the following angular dependence is obtained:

$$\frac{{\rm d}N}{{\rm d}\cos\theta_{\rm w}} = \frac{1}{2}\left[1 + h_{\rm w}(y)\mathcal{P}\cos\theta_{\rm w}\right] \tag{52}$$

where $h_{\rm w}(y)$ is also given in Table 1. It is evident that the charged lepton angular distribution is significantly more sensitive towards the polarization of t than the angular distributions of W and ν. The charged lepton is likely to be the less energetic lepton because its energy spectrum is softer than that of the neutrino. For large values of m_t the angular distribution of the less energetic lepton

$$\frac{{\rm d}N}{{\rm d}\cos\theta_<} = \frac{1}{2}\left[1 + h_<(y)\mathcal{P}\cos\theta_<\right] \tag{53}$$

is a more efficient analyser of top polarization than the angular distribution of neutrinos. For m_t in the range 150-200 GeV it is also better than the direction of W, c.f. Table 1.

The normalized distributions of leptons including first order QCD corrections can be cast into the following form:

$$\frac{{\rm d}N}{{\rm d}x_\ell\,{\rm d}\cos\theta_+} = \frac{1}{2}\left[\,{\rm A_l}(x_\ell) \,+\, \mathcal{P}\cos\theta_+\,{\rm B_l}(x_\ell)\,\right] \tag{54}$$

$$\frac{{\rm d}N}{{\rm d}x_\nu\,{\rm d}\cos\theta_0} = \frac{1}{2}\left[\,{\rm A}_\nu(x_\nu) \,+\, \mathcal{P}\cos\theta_0\,{\rm B}_\nu(x_\nu)\,\right] \tag{55}$$

Assuming the Standard Model V-A structure of the charged current the spectrum of the charged lepton vanishes at $x_\ell = 1$ and the spectrum of the neutrino does not vanish at $x_\nu = 1$. The latter spectrum is also significantly harder, see solid lines in Fig.8a-b. For V+A coupling the charged lepton and the neutrino energy spectra would be interchanged in comparison to the V-A case. In [39]

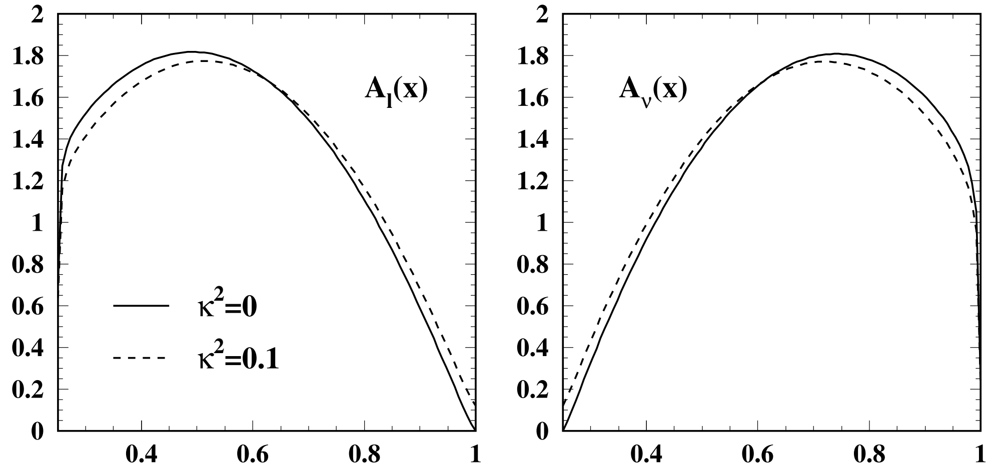

Figure 8: Energy distributions a) $A_l(x_\ell)$ of the charged lepton and b) $A_\nu(x_\nu)$ of the neutrino for the standard model V-A coupling ($\kappa^2 = 0$) and an admixture of V+A current ($\kappa^2 = 0.1$) for $y = 0.25$ and $\alpha_s = 0.11$.

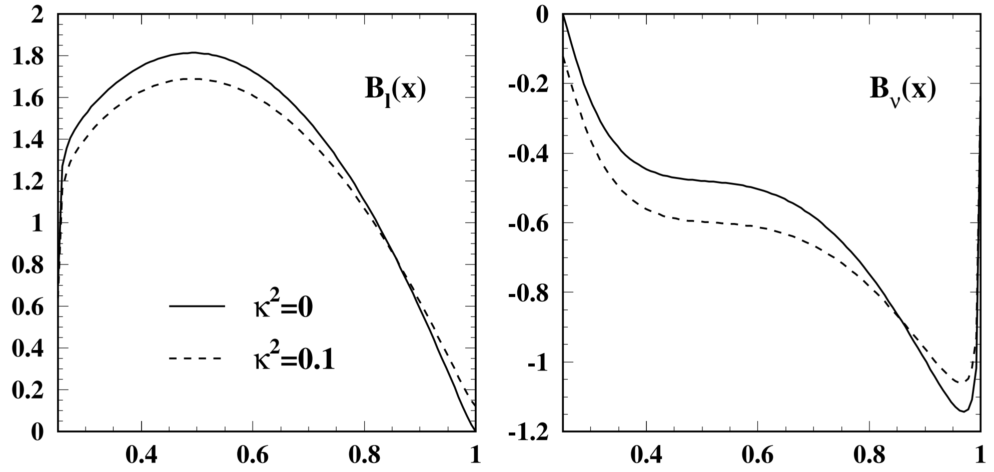

Figure 9: Angular-energy distribution functions in the Standard Model ($\kappa^2 = 0$) and for the admixture of V+A current ($\kappa^2 = 0.1$): a) $B_l(x_\ell)$ for the charged lepton and b) $B_\nu(x_\nu)$ for the neutrino, $y = 0.25$ and $\alpha_s = 0.11$.

effects have been studied of a small admixture of non-standard V+A current on distributions of leptons. The tbW vertex has been parametrized as

$$g_V\,\gamma^\mu \;+\; g_A\,\gamma^\mu\gamma_5 \tag{56}$$

where $g_V = (1+\kappa)/\sqrt{1+\kappa^2}$ and $g_A = (-1+\kappa)/\sqrt{1+\kappa^2}$ Hence $\kappa = 0$ corresponds to pure V-A and $\kappa = \infty$ to V+A. In Fig. 8a-b the lepton spectra are plotted corresponding to $\kappa^2 = 0.1$, see dashed lines. It can be seen that the deviations from the results of the Standard Model (solid lines) are rather small. In Fig.9 the functions $\mathrm{B_l}(x)$ and $\mathrm{B}_\nu(x)$ are shown as solid lines for y =0.25 and α_s =0.11 [39]. The effect of non-standard coupling defined in eq.(56) is much stronger for the polarization dependent distribution of neutrinos, see dashed lines in Fig.9 corresponding to $\kappa^2 = 0.1$ [39].

5 Polarized bottom and charm quarks

Polarization studies for heavy flavors at LEP[41, 42] and SLC[43] are a new and interesting field of potentially fundamental significance. According to the Standard Model $Z^0 \to b\bar{b}$ and $Z^0 \to c\bar{c}$ decays can be viewed as sources of highly polarized heavy quarks. The degree of longitudinal polarization is fairly large, amounting to $\langle P_b \rangle = -0.94$ for b and $\langle P_c \rangle = -0.68$ for c quarks [44]. The polarizations depend weakly on the production angle. QCD corrections to Born result are about 3% [45]. Therefore there is no doubt that the heavy quarks produced at the Z^0 resonance are polarized. However, this prediction still awaits a firm experimental verification. Unfortunately, these are hadrons rather than quarks which are registered in the detectors and the quantitative theoretical description of the spin transfer during the time development of a heavy quark jet is still lacking. Thus, it is not clear in which way the original high degree of polarization is reflected in the properties of jets containing heavy flavours. It has been proposed[46, 47] that non-zero helicities and chiralities of heavy quarks may result in non-zero values of two-particle momentum correlations for the most energetic particles in jets:

$$\Omega_{hel} = \mathbf{t}\cdot(\mathbf{k_1}\times\mathbf{k_2}) \qquad \text{and} \qquad \Omega_{chi} = \mathbf{t}\cdot(\mathbf{k}_+\times\mathbf{k}_-)$$

where for Ω_{chi} only particles of opposite electric charges are considered. However, in [43] a negative result has been recently reported of the search for the asymmetries in distributions of Ω_{hel} and Ω_{chi} No definite conclusion follows from this finding because no detailed theory exist relating these corelation functions with the primordial polarizations of the heavy quarks.

It seems more interesting to look for some signatures of the primordial polarization in those processes for which theoretical description is more reliable. Semileptonic decays of heavy flavors belong to this cathegory. Recently there has been considerable progress in the theory of the inclusive semileptonic decays of heavy flavor hadrons[48]. In the framework of Heavy Quark Effective Theory (HQET) and $1/m_Q$ expansion it has been shown that in the leading order the lepton spectra for the decays of hadrons coincide with those for the decays of free heavy quarks [49]. Away from the endpoint region there are no Λ_{QCD}/m_Q corrections to this result [49] and Λ^2_{QCD}/m^2_Q corrections have been calculated in [50, 51] for B mesons and in [51] for polarized Λ_b and Λ_c baryons. For some decays the results are similar to those of the well-known ACCMM model [52]. The corrections to charm decays are larger than for bottom and convergence of $1/m_Q$ expansion is poorer [53]. In [38] order α_s perturbative QCD corrections have been calculated to the angular and energy distributions of leptons in semileptonic decays of polarized charm and bottom quarks. Thus a complete theoretical description exists of the inclusive lepton spectra which should be accurate up to the level of few percent. Moreover, it has been pointed out [38, 54] that for semileptonic chanels not only the charged leptons but also the neutrinos can be registered as a missing energy-momentum. In consequence the sensitivity to the primordial polarization can be increased and simultaneously ambiguities in the process of jet fragmentation can be significantly reduced[54]. The real drawback is that due to hadronization the net longitudinal polarization of the decaying b and c quarks is drastically decreased. In particular these b quarks become depolarized which are bound in B mesons both produced directly and from $B^* \to B\gamma$ transitions[4]. The signal is therefore significantly reduced. Only those b's (a few percent) which fragment directly into Λ_b baryons retain information on the original polarization [55]. Polarization transfer from a heavy quark Q to the corresponding Λ_Q baryon is 100% [56] at least in the limit $m_Q \to \infty$. Thus, a large net polarization is

[4] B^* and D^* mesons from fragmentations of polarized b and c quarks retain some information on the primordial polarization. It is plausible that a quark with helicity -1/2 fragments into a state of helicity -1 more frequently than into that of helicity +1. In electromagnetic transitions, however this information is lost unless the polarization of real or virtual γ is measured. $D^* \to D\pi$ transitions might be more useful in this respect.

expected for heavy quarks in samples enriched with heavy Λ_b and Λ_c baryons. Since semileptonic decays are under control it is possible to measure these polarizations. Many new opportunities arise, polarization studies for other decay chanels among them. One of the most interesting may be studies of non-perturbative effects in fragmentation of bottom and charm quarks. Comparison of polarizations for Λ_b and Λ_c baryons can be instrumental in studying non-perturbative corrections to the spin transfer in fragmentation. This will be possible only if experimentalists can separate directly produced baryons from those from resonances. Assuming that this is possible and anticipating further progress in HQET as well as in perturbative QCD calculations one may expect that polarization studies for b systems at LEP will offer new opportunities to test the Standard Model. Recently, the ALEPH collaboration reported a preliminary result on Λ_b polarization $P_{\Lambda_b} = -0.30^{+.32}_{-.27} \pm .04$ [42]. This result which is well below theoretical expectations indicates that the sample may be contaminated with Λ_b's from decays of other beautiful baryons.

6 Acknowledgements

I would like to dedicate this work to Professor Kacper Zalewski on the occasion on his sixtieth birthday. Many of us owe Professor Zalewski a great debt for the stimulus and friendship he has given us over many years. I am particularly indebted to him for a help at a crucial stage in my academic life. I hope that this meeting has helped in some way to express that gratitude as well as our best wishes for the future.

References

[1] G. Alexander et al. (eds.), *Polarization at LEP*, CERN 88-06, Geneva 1988.

[2] S. Jadach and Z. Wąs, τ *Polarization at LEP*, in: G. Altarelli et al. (eds.), *Z Physics at LEP I*, CERN 89-08, vol.I, p.235, Geneva 1989.

[3] M. Woods, *Polarization at SLAC*, to appear in the proceedings of XI International Symposium on High Energy Spin Physics, SPIN'94, Sept.15-22, 1994, Bloomington, Indiana, USA.

[4] K. Abe et al. (SLD Collab.), Phys. Rev. Lett. 73 (1994) 25.

[5] V.S. Fadin and V.A. Khoze, JETP Lett. 46 (1987) 525; Sov. J. Nucl. Phys. 48 (1988) 309; Proc. 24th LNPI Winter School, Leningrad 1989, Vol.I, p.3.

[6] J.M. Strassler and M.E. Peskin, Phys. Rev D43 (1991) 1500.

[7] M. Jeżabek, J.H. Kühn and T. Teubner, Z. Phys. C56 (1992) 653.

[8] Y. Sumino, K. Fujii, K. Hagiwara, H. Murayama and C.-K. Ng, Phys. Rev. D47 (1993) 56.

[9] R. Harlander, M. Jeżabek, J.H. Kühn and T. Teubner, Phys. Lett. B346 (1995) 137.

[10] R. Harlander, M.Jeżabek and J.H. Kühn, in preparation.

[11] J.H. Kühn, in *Physics and Experiments with Linear* e^+e^- *Colliders*, eds. F.A. Harris et al., (World Scientific, Singapore, 1993), p.72.

[12] M. Jeżabek, Nucl. Phys. B (Proc. Suppl.) 37B (1994) 197.

[13] P.M. Zerwas (ed.), e^+e^- Collisions at 500 GeV: The Physics Potential, DESY Orange Reports DESY 92-123A, DESY 92-123B and DESY 93-123C.

[14] V.S. Fadin, V.A. Khoze and M.I. Kotsky, Z. Phys. C64 (1994) 45.

[15] J.H. Kühn, Acta Phys. Polon. B12 (1981) 347; Acta Phys. Austr. Suppl. XXIV (1982) 203.

[16] I.I. Bigi, Y.L. Dokshitzer, V.A. Khoze, J.H. Kühn and P.M. Zerwas, Phys. Lett. B181 (1986) 157.

[17] W. Kwong, Phys. Rev. D43 (1991) 1488.

[18] M. Jeżabek, and T. Teubner, Z. Phys. C59 (1993) 669.

[19] P. Igo-Kemenes, M. Martinez, R. Miquel and S. Orteu, in ref.[13], Part C, p.319.

[20] V.A. Khoze, in Proc. of the First Arctic Workshop on Future Physics and Accelerators, Saariselkä, Finland, Aug.21-26, 1994; preprint DTP/94-114, Nov. 1994.

[21] H. Murayama and Y. Sumino, Phys. Rev. D47 (1993) 82.

[22] F. Abe et al. (CDF Collab.), *Observation of Top Quark Production in $p\bar{p}$ Collisions*, FERMILAB-PUB-95/022-E.

[23] S. Abachi et al. (DØCollab.), *Observation of the Top Quark*, FERMILAB-PUB-95/028-E.

[24] J.H. Kühn and P.M. Zerwas, Phys. Reports 167 (1988) 321.

[25] W. Mödritsch and W. Kummer, Nucl. Phys. B430 (1994) 3;
W. Kummer and W. Mödritsch, preprint TUW-95-02, Jan. 1995.

[26] V.A. Khoze, L.H. Orr and W.J. Stirling, Nucl. Phys. B378 (1992) 413; Yu.L. Dokshitzer, V.A. Khoze, L.H. Orr and W.J. Stirling, Nucl. Phys. B403 (1993) 65.

[27] V.A. Khoze and T. Sjöstrand, Phys. Lett. B328(1994) 466.

[28] M. Ježabek and J.H. Kühn, Nucl. Phys. B314 (1989) 1.

[29] for a recent review see: M. Ježabek and J.H. Kühn, Phys. Rev. D48 (1993) 1910, erratum: D49 (1994) 4970.

[30] B.H. Smith and M.B. Voloshin, Phys. Lett. B340 (1994) 176.

[31] H. Überall, Phys. Rev. 119 (1960) 365.

[32] K. Melnikov and O. Yakovlev, Phys. Lett. B324 (1994) 217.

[33] Y. Sumino, Tokyo Univ. PhD thesis, 1993 (unpublished).

[34] J.H. Kühn, A. Reiter and P.M. Zerwas, Nucl. Phys. B272 (1986) 560.

[35] A. Czarnecki and M. Ježabek, Nucl. Phys. B427 (1994) 3.

[36] M. Ježabek and J.H. Kühn, Nucl. Phys. B320 (1989) 20.

[37] A. Czarnecki, M. Ježabek and J.H. Kühn, Nucl. Phys. B351 (1991) 70.

[38] A. Czarnecki, M. Ježabek, J.G. Körner and J.H. Kühn, Phys. Rev. Lett. 73 (1994) 384.

[39] M. Jeżabek and J.H. Kühn, Phys. Lett. B329 (1994) 317.

[40] F.J. Gilman and R. Kauffman, Phys. Rev. D37 (1988) 2678.

[41] B. Mele, Mod. Phys. Lett. A9 (1994) 1239.

[42] P. Roudeau, *Heavy Quark Physics*, in proceedings of XXVII Int.Conf. on High Energy Physics, 20-27 July 1994, Glasgow, Scotland.

[43] K. Abe et al. (SLD Collab.), Phys. Rev. Lett. 74 (1995) 1513.

[44] J.H. Kühn and P.M. Zerwas, in *Heavy Flavours*, eds. A.J. Buras and M. Lindner, (World Scientific, Singapore, 1992), p.434.

[45] J.G. Körner, A. Pilaftsis and M.M. Tung, Z. Phys. C63 (1994) 575.

[46] O. Nachtmann, Nucl. Phys. B127 (1977) 314.

[47] A.V. Efremov et al., Phys. Lett. B284 (1992) 394; ibid B291 (1992) 473.

[48] For a review see: I. Bigi, in these proceedings.

[49] J. Chay, H. Georgi and B. Grinstein, Phys. Lett. B247 (1990) 399.

[50] I. Bigi, M. Shifman, N. Uraltsev and A. Vainshtein, Phys. Rev. Lett. 71 (1993) 496; B. Blok, L. Koyrakh, M. Shifman and A. Vainshtein, Phys. Rev. D49 (1994) 3356.

[51] A.V. Manohar and M.B. Wise, Phys. Rev. D49 (1994) 1310.

[52] G. Altarelli et al, Nucl. Phys. B208 (1982) 365.

[53] B. Blok, R.D. Dikeman and M. Shifman, preprint TPI-MINN-94/23-T.

[54] G. Bonvicini and L. Randall, Phys. Rev. Lett. 73 (1994) 392.

[55] J.D. Bjorken, Phys. Rev. D40 (1989) 1513.

[56] F.E. Close, J.G. Körner, R.J.N. Phillips and D.J. Summers, J. Phys. G18 (1992) 1716.